https://rbgeomorfologia.org.br/
ISSN 2236-5664

Revista Brasileira de Geomorfologia

v. 27, nº 2 (2026)

http://dx.doi.org/10.20502/rbg.v27i2.2676

Research Article

Susceptibility of River Basins to Flooding in Contact Zones Between Mountain Ranges and Coastal Plains: contributions of morphometric indices in the tropical Atlantic region of Southeastern Brazil

Suscetibilidade de Bacias Hidrográficas a Inundações em Zonas de Contato entre Faixas Montanhosas e Planícies Litorâneas: contribuições de índices morfométricos na região tropical atlântica no Sudeste do Brasil

Marcus Vinícius Oliveira Sartório [1] and Antônio Pereira Magalhães Júnior [2]

[1] Universidade Federal de Minas Gerais, Instituto de Geociências, Belo Horizonte, Brazil. marcus.sartorio@gmail.com
ORCID: https://orcid.org/0000-0003-1307-8782

[2] Universidade Federal de Minas Gerais, Instituto de Geociências, Belo Horizonte, Brazil.
antonio.magalhaes.ufmg@gmail.com
ORCID: https://orcid.org/0000-0002-5327-3729

Received: 17/02/2025; Accepted: 02/06/2026; Published: 21/06/2026

Abstract: The analysis of morphometric parameters has been widely employed to assess flood susceptibility; however, at broader scales, it tends to homogenize and generalize results, concealing relevant local differences. This study aims to investigate flood susceptibility using fifteen morphometric parameters in a GIS environment, at scales ranging from basins and sub-basins up to the sixth order, located in the northern Mantiqueira range/coastal plain of Espírito Santo, Brazil. The methodological approach enabled comparative analyses and a more detailed assessment of morphometric susceptibility, while also providing a more consistent regional comprehension. Additionally, the results were related to the rainfall regime using the CHELSA 1.2 global precipitation model, which allowed for the identification of more critical sub-basins. The analyses highlight the relevance of parameters such as area, altimetric amplitude, perimeter, and main channel slope in defining areas more susceptible to flooding. In mountainous and small-sized basins, such characteristics may be more determinant than precipitation itself in intensifying surface runoff. The sub-basin level analysis revealed local susceptibility patterns, emphasizing the concentration of critical areas in the middle and lower courses of the Santa Maria River basin and the widespread distribution in the Jucu River basin, as well as the asymmetry observed on the right margin of the main channels of both basins.

Keywords: Hydrogeomorphology; Hydrogeography; Quantitative geomorphology; Drainage morphometry.

Resumo: A análise de parâmetros morfométricos tem sido amplamente empregada para avaliar a suscetibilidade a eventos de inundação; contudo, em grandes escalas, tende a homogeneizar e generalizar os resultados, ocultando diferenças locais relevantes. Este artigo tem como objetivo investigar a suscetibilidade a inundações por meio de quinze parâmetros morfométricos aplicados em ambiente SIG, em escalas que abrangem bacias e sub-bacias até a sexta ordem, situadas na faixa Mantiqueira setentrional/planície litorânea do Espírito Santo. A abordagem metodológica possibilitou análises comparativas e maior detalhamento da suscetibilidade morfométrica, além de oferecer uma compreensão regional mais consistente. Complementarmente, os resultados foram relacionados ao regime pluvial por meio do modelo global de precipitação CHELSA 1.2, o que permitiu identificar sub-bacias mais críticas. As análises evidenciam a relevância de parâmetros como área, amplitude altimétrica, perímetro e declividade do canal principal na definição de áreas mais suscetíveis a inundações. Em bacias montanhosas e de pequenas dimensões, tais características podem ser mais determinantes que a própria precipitação na intensificação do escoamento superficial. A análise em nível de sub-bacia revelou padrões locais de suscetibilidade, destacando a concentração de áreas críticas no médio e baixo curso da bacia do rio Santa Maria e a ampla distribuição na bacia do rio Jucu, além da assimetria observada na margem direita dos canais principais de ambas.

Palavras-chave: Hidrogeomorfologia; Hidrogeografia; Geomorfologia quantitativa; Morfometria de drenagem.

1. Introduction

Floods are the primary drivers of natural disasters in coastal basins, both at national and global scales (WMO, 2016; UNDRR, 2020). Furthermore, river floodplains and coastal areas exhibit a clear trend toward human concentration and expansion (Small; Nicholls, 2003; Rentschler et al., 2022), which, combined with the inherent natural susceptibility of these environments to flooding, renders them particularly vulnerable to risks and damages. Rainfall intensity and frequency are frequently identified as decisive factors in flood generation, commonly associated with the extreme climatic events that reflect recent multi-decadal climate oscillations (IPCC, 2021; UNDRR, 2020). Conversely, the dynamics of these events are intrinsically linked to the morphometric configuration of river basins. This relationship has motivated the development of quantitative parameters widely investigated since the 1940s, notably through the seminal works of Horton (1945) and Strahler (1952). Within this context, analyzing the morphometric properties of fluvial systems is essential to understanding how different basins hydrologically respond to meteoric events, allowing for the correlation of drainage network shape and structure with flood magnitude and velocity (Borga et al., 2008).

In the risk equation, assessing susceptibility to these events has advanced significantly through the application of geoprocessing techniques to morphometric studies. Over the past few decades, a vast body of literature has accumulated regarding the role of fluvial morphometry in controlling flood occurrence and intensity. Studies such as those by Ozdemir and Bird (2009), Romshoo, Bhat, and Rashid (2012), Bhatt and Ahmed (2014), Abuzied et al. (2016), Fenta et al. (2017), Bhat et al. (2019), and Alam, Ahmed, and Sammonds (2021) demonstrate how fluvial morphometry analysis has progressed alongside emerging geoprocessing and remote sensing technologies.

However, macro-scale morphometric analysis of river basins imposes severe analytical limitations, since very extensive basins tend to conceal important hydrogeomorphological differences that locally favor the development of these events. The inherent heterogeneity of these large hydrological systems makes it difficult to accurately represent hydrological and morphometric processes, causing morphometric variables to assume average and generalized values that do not reflect the true dynamics of specific sectors (Mendiondo; Tucci, 1997; Sirangelo, 2014). This scale limitation leads to a generalization of susceptibility to flooding, since the analysis of a main basin draining varied lithologies and reliefs masks the diversity of critical values frequently found in its lower-order channels. To overcome this bias, the scientific literature indicates that detailed analysis at the sub-basin and micro-basin scale is fundamental. This is because these areas drain more homogeneous substrates, act as the main feeders of macro-fluvial systems, and more accurately reflect vulnerability to extreme events (Pinto et al., 2016; Cherem, 2008).

Thus, this article aims to investigate the susceptibility to flooding in river basins of varying spatial scales located between the Mantiqueira Range and the coastal plain of southeastern Brazil, based on morphometric parameters. This approach allowed for comparative analyses, a deeper understanding of morphometric susceptibility, and a broader regional understanding of an area significantly affected by these events. Complementarily, morphometric susceptibility was related to rainfall patterns using the CHELSA 1.2 global precipitation model (Karger et al., 2017), aiming to identify the most critical sub-basins.

The coastal basins of the northern Mantiqueira ridge/coastal plain region in Southeastern Brazil are preferential zones for intense and recurrent flooding, characterized by a seasonal rainfall regime and strong orographic influence (Nascimento, 2017). Historical floods date back to 1922, 1938, 1940, 1960, and 1979, a period when urban occupation along riverbanks and coastal plains was still limited. More recent well-documented events, in 1997, 2008, 2013, 2020 and 2024, encountered environments characterized by high natural vulnerability and substantial risk driven by aggressive urban expansion over recent decades (Silva, 2010; D'Alcântara, 2012; Deina; Coelho, 2015; INMET, 2024). Historical floods date back to 1922, 1938, 1940, 1960, and 1979, a period when urban occupation along riverbanks and coastal plains was still limited. More recent well-documented events in 1997, 2008, 2013, 2020, and 2024 encountered environments characterized by high natural vulnerability and substantial risk driven by aggressive urban expansion over recent decades (Silva, 2010; D'Alcântara, 2012; Deina; Coelho, 2015; INMET, 2024). Although site-specific studies exist for some basins within the study area, regional-scale research implementing comparative analyses of hydrogeomorphological dynamics remains scarce. This scarcity creates critical gaps and highlights the need for investigations that deepen the understanding of both natural and anthropogenic factors influencing fluvial dynamics in this region.

2. Study area

The area corresponds to two sixth-order basins: the Santa Maria River (BHSM), with 1791.2 km², and the Jucu River (BHJC), with 2129.4 km², located on the south-central coast of the state of Espírito Santo, in the Southeast Atlantic hydrographic mesoregion (Figure 1). The basins have an altimetric amplitude that reaches 1889 m in their westernmost portion, with drainage axes aligned NW-SE, draining directly into the ocean, and drainage divides located in the northern portion of the Mantiqueira Range. On the reverse side of the basins is the southern portion of the Doce River basin, which drains an area of 83,400 km² and limits the coastal basins in such a way that the drainage divides are positioned parallel to the coastline at an average distance of 84 km. This characteristic has a decisive influence on hydrological behavior, forming coastal basins with reduced flow volumes compared to other surrounding basins.

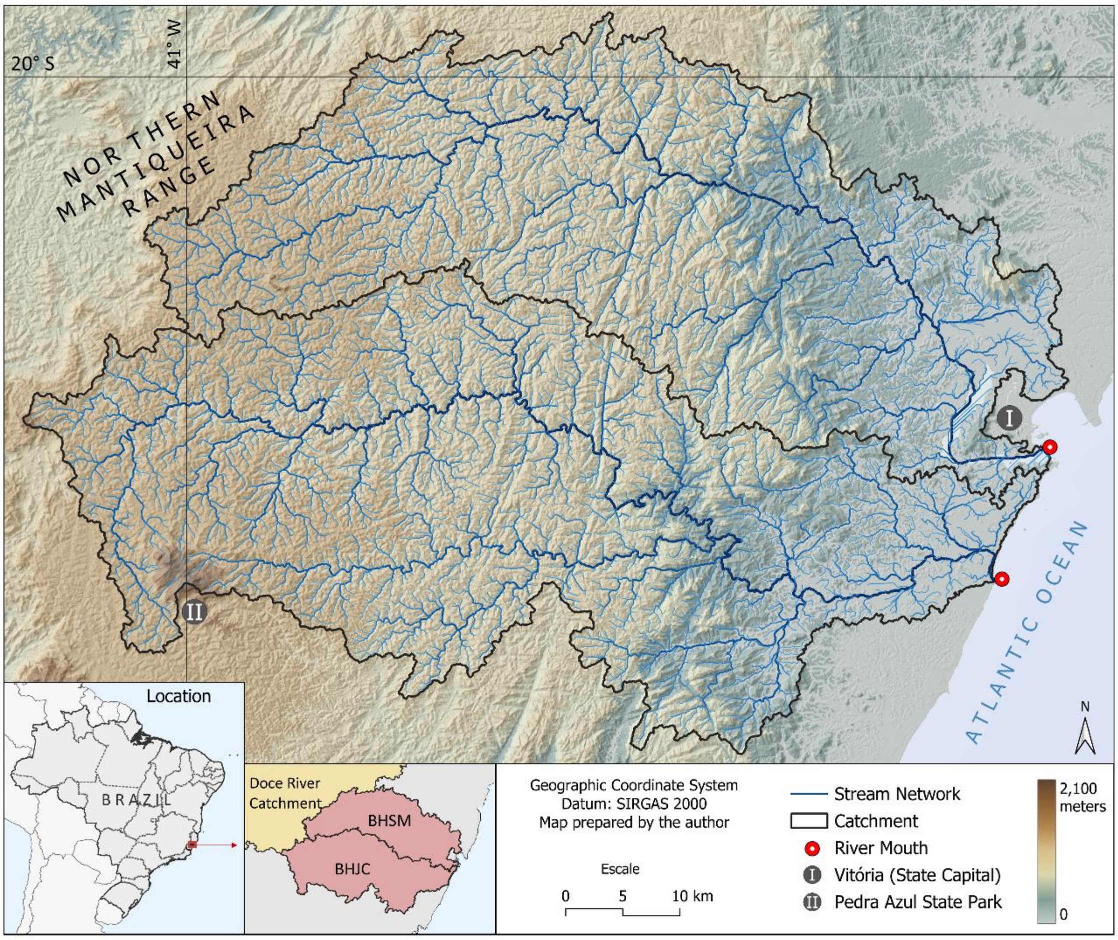

Figure 1. Location of the Santa Maria River (BHSM) and Jucu River (BHJC) basins. Map prepared by the author.

The basins studied are located within two geological compartments. One corresponds to the Precambrian basement, composed of plutonic and metamorphic rocks, to the west. The other refers to the Cenozoic sedimentary deposits that occur on the plateaus of the Barreiras Formation, of Neogene origin (previously included in the Tertiary), and in the Quaternary deposits downstream of the basins, on the coast and in the floodplains. The headwaters of the basins are located in the far north of the Mantiqueira range, which forms a mountain range parallel to the southeastern coast of Brazil (WSW-ENE direction). The Range is situated within the context of a Elevated Passive Continental Margin, forming a transition between the coastal plain and the continental interior (Silva et al. 1987; Calegari et al., 2021). Although there is no sharp escarpment associated with the regional drainage divides, a substantial drop in elevation is observed down to the regional base level, occurring in a stepped manner in the Precambrian basement. This basement is formed by a complex association of igneous and metamorphic rocks, related to the Araçuaí and Ribeira orogen belts of the Brasiliano event (Almeida, 1977).

The topographic contrast between the mountainous zone and the coastal plains exerts a relevant influence on rainfall distribution and volume in the region, as well as on fluvial regimes. The Mantiqueira Range represents an obstacle to the circulation of polar fronts and other atmospheric circulation mechanisms, locally increasing rainfall volumes (IBGE, 1977; Antongiovanni; Coelho, 2005; Silva et al., 2011).

The mean annual precipitation in the study area ranges from 973 to 1933 mm, with an average of 1394 mm (Figure 2). The highest accumulations occur near the headwaters, with values around 1400 to 1600 mm yr^{-1}, exceeding 1900 mm yr^{-1} in the Jucu River basin. Conversely, in the coastal portion, which encompasses the downstream areas of the catchments, precipitation rates range between 1100 and 1300 mm yr^{-1} (Figure 3). In a regional context, Nunes, Vicente and Candido (2009) point out that one of the main problems faced is concentrated precipitation associated with the availability of relative air humidity driven by maritime influence. Rainfall concentration may also explain a shift in interannual precipitation variability in the southeastern region of the country, as indicated by Vasconcellos (2008) and Carvalho and Jones (2009), which can result in wetter summers and drier winters, thereby potentiating extreme meteorological events in the area.

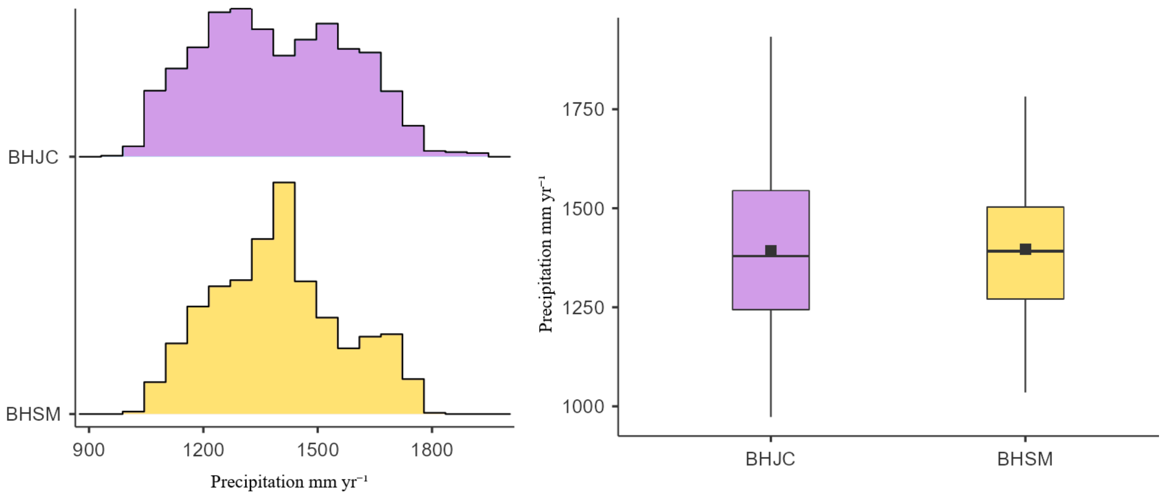

Figure 2. Distribution of average annual precipitation for the years 1979 and 2013 extracted from CHELSA v1.2 (Karger et al. 2017) for BHSM and BHJC. Frequency histograms are presented on the left and boxplots indicating interquartile ranges, mean and median are on the right.

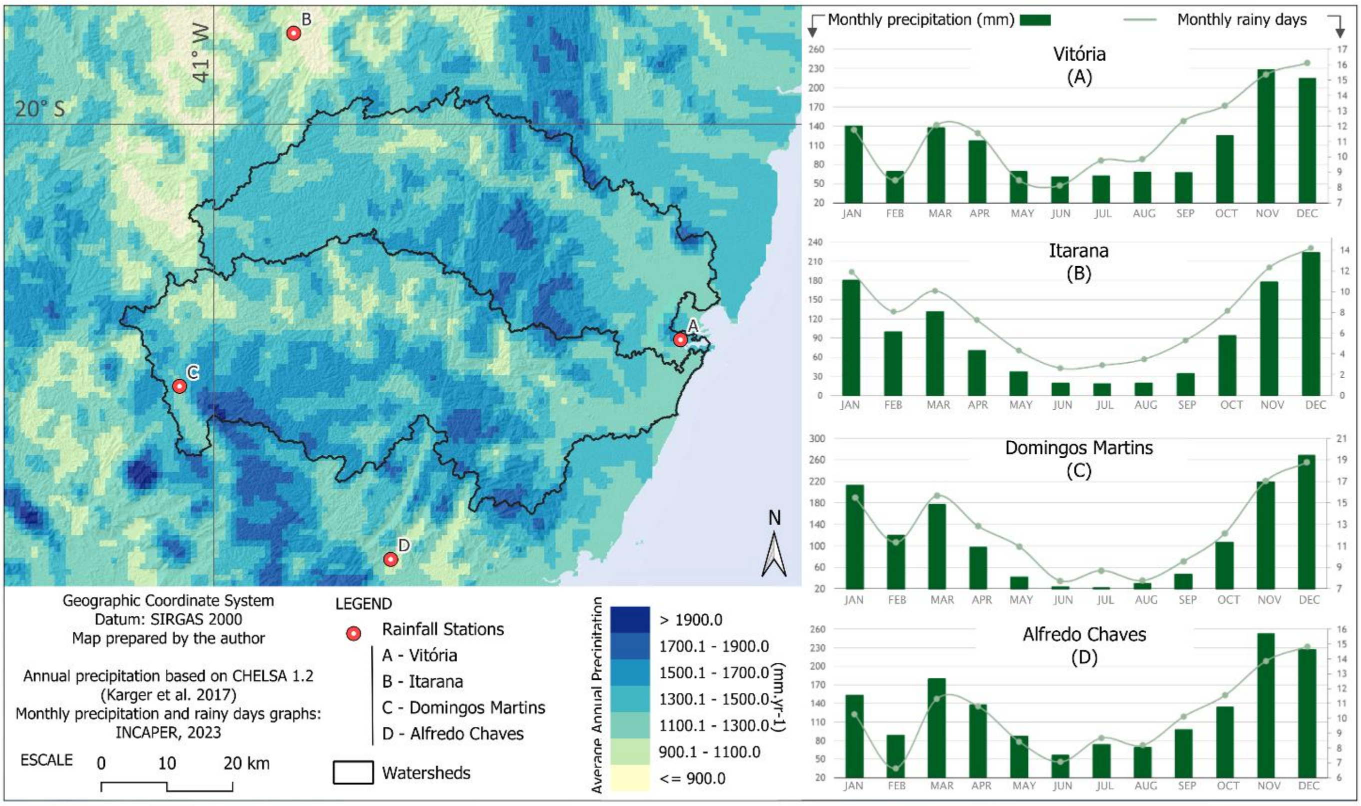

Figure 3. Average annual precipitation based on CHELSA 1.2 (Karger et al., 2017) and average monthly precipitation and monthly rainy days at rain gauge stations in the INCAPER study area (2023) – Graphs of historical series from 1984 to 2014. Map prepared by the author.

3. Materials and Methods

3.1. Morphometric analysis

Since the early studies by Horton (1945), Strahler (1952), Miller (1953) and Schumm (1956), many researchers have focused on the main parameters that influence catchment hydrodynamics. Broadly, catchments are the most adequate analytical unit for geomorphological analyses, integrating hillslope processes, plains, and fluvial channels (Christofoletti, 1999; Magalhães Júnior; Lopes, 2022), which can be quantitatively evaluated based on their attributes and the relationships between these attributes.

Morphometric parameters encompass a series of analyses based on two distinct time scales. The first corresponds to long-term analyses of catchment genesis and evolution (thousands/millions of years), such as their lithostructural and tectonic conditioning, and river captures, responsible for shaping the relief. The second time scale encompasses analyses of the characterization of recent/current fluvial dynamics with a view to understanding how morphology acts on the hydrological events that occur within them. This second scale is the one addressed in this article, considering parameters that are more closely related to the current dynamics of floods.

Even though the application of morphometric parameters in the investigation of fluvial floods has been operational for more than half a century, there is no consensus in the literature on how many parameters researchers should use to more accurately assess the flood potential in catchments, making it difficult to compare studies, even those dealing with the same area (Adnan et al., 2020). However, one of the critical steps in choosing parameters, as highlighted by Tehrany, Jones, and Shabani (2019), is the selection of the most relevant and influential conditioning factors in flood generation. This is because, as observed in the studies by Abdel-Fattar et al. (2017) and Shen et al. (2017), redundancy does not stem from the abundance of parameters itself, but from the use of redundant parameters within the same study.

However, there are some fundamental parameters that reveal an interdependence between drainage network characteristics, hydrological responses, and natural susceptibility to flooding. One of the basic parameters is the fluvial hierarchy (Strahler, 1952), which involves the classification of watercourses according to the hierarchy of tributaries. Based on this hierarchy, it is possible to identify and map nested catchments of each stream order, favoring a sectorization capable of indicating areas with greater or lesser morphometric susceptibility to fluvial flooding at different scales. The other parameters were also extracted and calculated according to Strahler's (1952) classification.

Based on the literature review on the subject, 15 attributes and parameters were listed (Table 1) in order to understand the morphometric susceptibility to fluvial flooding in the catchments, deriving the values of these parameters through the application of different mathematical procedures in a GIS (Geographic Information System) environment. The values obtained for the Isp and Tc parameters are inversely related to fluvial flooding generation potential, whereas the others are directly related.

Table 1. Morphometric attributes and parameters related to flood development selected for this analysis.

Attribute / Parameter	Expression	Definition	Reference
Stream Order (Su)	$1, 2, 3 \ldots n$	Indicates the hierarchical rank and branching complexity of the basin channels according to the Strahler (1952) classification. It provides a means to assess the hierarchical branching pattern of streams within a watershed, having a direct relationship with water discharge capacity and being fundamental for identifying sub-basins. The extraction of geomorphic parameters is intrinsically conditioned by the stream order.	Strahler (1952)
Stream Number (Nu)	$Nu = N1 + N2 \ldots + Nn$	A linear attribute that indicates the total number of stream segments of all orders within each watershed according to Su.	Horton (1945)
First-order stream frequency (Fs1)	$Fs1 = \frac{Nu1}{Nu}$	A parameter that relates the number of first-order streams to the total number of streams in the basin. A high number of first-order streams reflects a rapid flow of water out of the basin, indicating that more water is being discharged as surface runoff than is being infiltrated into the soil.	Morisawa (1962)
Main channel length (Lm)	$[km]$	A linear attribute that indicates the distance along the longest watercourse from the mouth to the head of the channel.	Schumm (1956)
Stream length (Lu)	$Lu = L1 + L2 \ldots + Ln$	A linear attribute corresponding to the sum of the lengths of all individual stream segments in the catchment.	Horton (1945)
Main stream sinuosity (Si)	$Si = \frac{Lm}{Lv}$	A parameter that relates the length of the main channel (*Lm*) to the down-valley distance (straight-line distance) between its endpoints (*Lv*). It is a measure of how much the channel deviates from a straight line, representing structural and lithological controls over drainage, as well as the flow energy.	Christofoletti (1980)
Basin area (A)	$[km^2]$	An attribute that corresponds to the total area of the catchment bounded by its topographic divides, projecting the catchment area available for runoff.	Schumm (1956)
Basin perimeter (P)	$[km]$	An attribute that corresponds to the total length of the catchment boundary.	Horton (1945)
Form factor (F)	$\mathrm{F} = \frac{A}{Lm^2}$	A dimensionless parameter corresponding to the ratio between the basin area (*A*) and the square of its basin length (*Lm*).	Horton (1932)
Compactness coefficient (Kc)	$Kc = 0{,}28\, x \frac{P}{\sqrt{A}}$	A dimensionless parameter that relates the shape of the basin to that of a circle of equivalent area. Values closer to unity (1.0) correspond to perfectly circular basins, which are more susceptible to flooding, while higher values indicate an elongated shape that favors runoff translation.	Schumm (1956)
Stream Frequency (Fs)	$\mathrm{Fs} = \frac{Nu}{A}$	A parameter corresponding to the ratio between the total number of stream (*Nu*) segments and the basin area (*A*). It serves as an indicator of the hydrological response to surface runoff, whereby high *Fs* values indicate a higher volume of surface runoff and reduced infiltration capacity.	Horton (1945); Patton e Baker (1976)
Drainage Density (Dd)	$Dd = \frac{Lu}{A}$	A parameter that relates the total length of all stream channels to the drainage basin area. High *Dd* values constitute a significant indicator of greater surface runoff volumes and rapid flood peaks, often associated with impermeable subsurface and mountainous terrain.	Horton (1932, 1945)

Basin Relief (R)	$R = Hmax - Hmin$	An attribute corresponding to the difference in elevation between the highest and lowest points (mouth) of the basin.	Schumm (1956)
Relief Ratio (Rr)	$Rr = \frac{R}{Lm}$	A dimensionless parameter corresponding to the ratio between the basin relief (*R*) and the maximum stream length (*Lm*) measured parallel to the principal drainage line. It provides an assessment of the overall steepness of a drainage basin and acts as a significant indicator of surface runoff velocity, flow gradients, and erosion status, which ultimately influence hydrological behavior.	Schumm (1956)
Ruggedness Number (Rn)	$Rn = R * Dd$	A dimensionless parameter representing the product of drainage density (*Dd*) and basin relief (*R*). It indicates the steepness of slopes and hydraulic transmissivity. *Rn* is characteristically high in basins with steep, long slopes, creating a highly susceptible environment that favors erosion, quick peak flows, and flash floods.	Patton e Baker (1976)
Time of Concentration (Tc)	$Tc = \left(0,87\ \frac{Lm^3}{H}\right)^{0,385}$	A hydrologic parameter corresponding to the maximum time required for water to travel from the most distant point of the catchment to the mouth. *Tc* is a fundamental parameter to estimate the peak discharge potential of a catchment; wherein higher *Tc* values imply a lower probability of sudden peak discharges and attenuated flood hydrographs.	Kirpich, 1940

3.2. DEM processing and sub-catchment extraction

Topographic analysis techniques were applied to a DEM (Digital Elevation Model) to extract quantitative information on the morphometric configuration of fluvial systems. The utilized model was the Copernicus-DEM, obtained through the European Commission's online platform – PANDA, featuring TanDEM-X project data at a spatial resolution of 1 *ArcSec*. The choice of this DEM is justified by its higher accuracy compared to other 1-arc-second models, as compared by Guth and Geoffroy (2021).

The maps were created using the free and open-source software QGIS 3.22, in the UTM coordinate system and SIRGAS 2000 reference datum, zone 24k. The TopoToolbox 2.4 toolset, a package of tools for quantitative topographic analysis developed for the MATLAB environment (Schwanghart; Scherler, 2014), was also used.

To make the DEM hydrologically consistent, a pre-processing routine was performed in TopoToolbox 2.4, using the 'carve' algorithm, which seeks to remove spurious depressions or flat regions that hinder the correct delineation of the upstream drainage area and compromise all subsequent metric extraction steps. Subsequently, the 'imposemin' [0.0001] algorithm was applied, rendering the derived drainage to decrease monotonically downstream along the longitudinal profile of the rivers. Furthermore, the Copernicus DEM with non-discretized values was chosen.

The delineation of the catchment perimeter was performed using the TopoToolbox 2.4 'drainagebasins' algorithm, which determines catchments based on a flow direction matrix. From this data, a 'streamorder' matrix was generated, allowing the generation of catchments based on the stream-order classification of their main channel, according to the stream ordering of Strahler (1952). The output of this algorithm generated catchments and sub-catchments (Figure 4), which, in turn, enabled the quantification of several attributes, such as the Basin area (A) and the Basin Relief (R) of catchments and sub-catchments up to the sixth order.

In this study, first- and second-order catchments were not considered due to three factors: a) the low frequency of fluvial flooding in headwater catchments; b) the difficulty in obtaining significant data for parameters in catchments with an areal and drainage extent of only a few m²; and c) the scale limitation of the data extracted from the 1 *ArcSec* DEM.

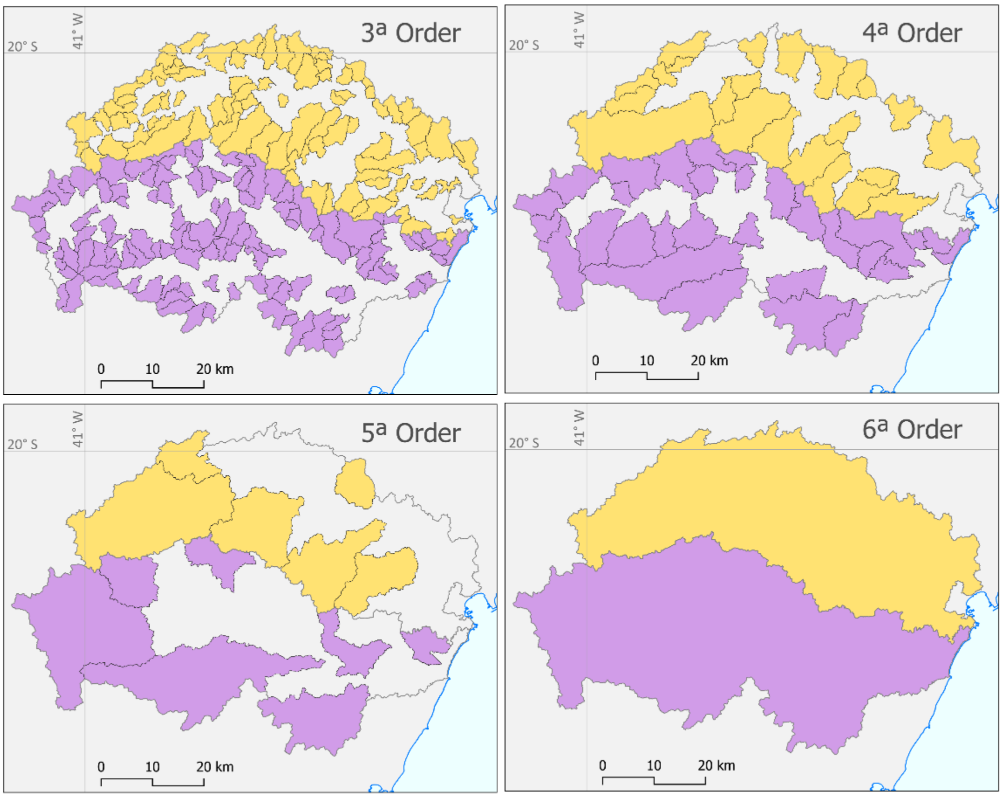

Figure 4. Distribution of the catchments and sub-catchments in the study area classified from third- to sixth-order according to the stream ordering of Strahler (1952). Map prepared by the author.

3.3. Metric extraction, statistical treatment, and definition of susceptibility classes

To identify morphometric susceptibility, several attributes were extracted, which, correlated among themselves and with the relief, generating the morphometric parameters of the catchments and sub-catchments (Table 1). The extraction of hypsometric attributes such as maximum elevation (Hmax), minimum elevation (Hmin), and Basin Relief (R) was performed using the 'Zonal Statistics' algorithm in QGIS 3.22 on the pre-processed and hydrologically consistent DEM. The main channels of the catchments were extracted using the 'trunk' algorithm of TopoToolbox 2.4, based on the catchment hierarchical classification, generating main channels for each sub-catchment up to the sixth-order.

The comparison of absolute values of each parameter across different catchments or sub-catchments can generate inconsistencies in the results, due to the particularities of each system and the use of different scales. For a consistent comparison, the derived values of the chosen morphometric parameters, corresponding to each catchment, were converted to a new scale for susceptibility assessment.

To choose the number of classes, each parameter was initially subjected to an exploratory data analysis as a normal distribution test to identify the behavior of the data distribution. Based on the analysis, the central tendency (mean and median) and the dispersion (range, quartiles of the dataset, variance, and standard deviation as measures of spread) were identified. This procedure made it possible to understand the data distribution behavior of each parameter in order to choose the scale classification criterion and the most adequate number of classes.

As a result of the distribution analysis performed in the Jamovi 2.3.28 (2022) software, using the Shapiro-Wilk test (Shapiro; Wilk, 1965), out of the 15 parameters, only the First-order stream frequency (Fs1) showed a normal distribution in third-order catchments. In fourth-order catchments, only the Basin Relief (R), First-order stream frequency (Fs1), Compactness coefficient (Kc), and Ruggedness Number (Rn) indicated a normal distribution, whereas for fifth-order catchments all morphometric parameters indicated a p-value > 0.05, which was already expected due to the limitation of normality tests for small samples (Razali; Wah, 2011). The normality test was not applied to sixth-order catchments (Table 2).

Table 2. Distribution of the morphometric data obtained for third- to fifth-order catchments. Normality significance p-values extracted using the Shapiro-Wilk test. Highlights indicate the values with normal distribution.

Parameter	*A*	*P*	*R*	*Lm*	*Si*	*Nu*	*Lu*	*Fs1*	*Kc*	*F*	*Dd*	*Fs*	*Rr*	*Rn*	*Tc*
3ª order	< 0,001	< 0,001	< 0,001	< 0,001	< 0,001	< 0,001	< 0,001	0,006	< 0,001	< 0,001	< 0,001	< 0,001	< 0,001	< 0,001	< 0,001
4ª order	< 0,001	< 0,001	0,117	< 0,001	< 0,001	< 0,001	< 0,001	0,063	0,423	0,002	< 0,001	< 0,001	< 0,001	0,046	< 0,001
5ª order	0,008	0,145	0,095	0,047	0,874	0,005	0,007	0,031	0,811	0,342	0,006	0,129	0,018	0,092	0,077

Based on these tests, in which most data exhibit a p-value < 0.005, it was determined that the median and interquartile ranges are the most adequate measures of spread to evaluate the obtained dataset, so that the classes are adjusted according to the corresponding quartile. With the number of intervals and limit values identified, the classification of each interval was performed according to its relative degree of susceptibility. For this purpose, it was necessary to verify how each parameter relates - positively or negatively - to the potential for generating fluvial flooding, such that each value is associated with a point scale:

a) very high = 4; b) high = 3; c) moderate = 2; d) low = 1

Finally, the cumulative value of the individual scores for each parameter according to the scale was used to assess the degree of morphometric susceptibility of the catchment. Thus, the minimum point value that each catchment can achieve is equal to 'n' evaluated parameters, whereas the maximum is 'n' x 4, further considering that each parameter carries the same weight.

The catchments were labeled with an identification code to facilitate the visualization of the results for lower-order catchments, where the first number corresponds to the stream-order according to Strahler (1952), followed by the name of the main catchment: "SM" for BHSM and "JC" for BHJC. Finally, numbering followed in sequential order, as presented below:

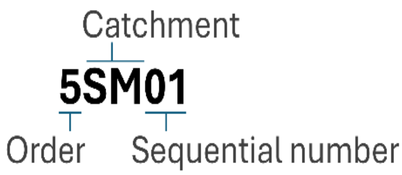

3.4. Precipitation data integration

After mapping the morphometric susceptibility, the integration of new information layers regarding precipitation and the location of urban and rural communities was performed, forming a more detailed composition of the sub-catchments considered at higher risk. This composition was achieved by overlaying the mean precipitation values for each sub-catchment onto the morphometric susceptibility mapping, such that the susceptibility to fluvial flooding result considered both the morphometric susceptibility class value and the precipitation class value. Following the same class adjustment used for the morphometric parameters, the four precipitation classes were defined based on the minimum and maximum values, as well as the quartiles and interquartile ranges of the study area.

For this purpose, data from the CHELSA V1.2 model - Climatologies at High resolution for the Earth Land Surface Areas were utilized, which is a high-resolution global climatic dataset referring to the 1979 to 2013 historical series, made available in raster format with a spatial resolution of 30 ArcSec (KARGER et al., 2017). Since the original database provides the climatological normals in monthly averages, the twelve layers were summed using the Map Algebra tool (Raster Calculator) in the QGIS 3.22 software, generating a new raster surface representative of the mean annual precipitation. Finally, to extract the mean precipitation value corresponding to the drainage area of each specific sub-catchment, the Zonal Statistics algorithm was employed, allowing for cross-tabulation and integration with the morphometric indices.

4. Results and discussion

4.1. Morphometric susceptibility in sixth-order catchments

The BHSM and BHJC possess important hydrographic similarities as they present similar geological-geomorphological conditions (Table 3).

Table 3. Basic attributes of the Santa Maria and Jucu river catchments.

Attributes	BHSM	BHJC
Area (km²)	1791.21	2129.46
Perimeter (km)	466.39	483.88
Main channel length (km)	143.22	172.51
Basin Relief (m)	1446.27	1889.10
Stream Number	2354	2771
Number of first-order streams	1812	2142
Number of second-order streams	419	477
Number of third-order streams	93	114
Number of fourth-order streams	23	30
Number of fifth-order streams	6	7
Number of sixth-order streams	1	1

The headwaters of the main streams are located in the mountainous relief of the northern portion of the Mantiqueira Range, also draining the Patamares Escalonados do Sul Capixaba, in a predominant NW-SE direction, and the coastal plains in the downstream areas. The BHJC stands out in relation to the BHSM for having a higher number of parameters favorable to the development of fluvial flooding (Table 4). The BHJC has an area 18.9% larger than the BHSM, which directly impacted parameters associated with its dimension, such as A, P, Lm, Nu, Lu, making it more susceptible to fluvial flooding.

In absolute terms, both catchments possess topographic characteristics prone to the generation of fluvial flooding given the steep slope associated with indicators that point to high surface runoff as Stream Frequency (Fs) and Drainage Density (Dd), and time of concentration of the flows as Form factor (F) and Compactness coefficient (Kc), in addition to the history of recurrent extreme fluvial flooding.

Table 4. Morphometric attributes and parameters of the Santa Maria and Jucu river catchments. Grey highlights indicate the parameters most favorable to the development of fluvial flooding, based on the definitions presented in Table 1.

Parameter	*A*	*P*	*R*	*Lm*	*Si*	*Nu*	*Lu*	*Fs1*	*Kc*	*F*	*Dd*	*Fs*	*Rr*	*Rn*	*Tc*
BHSM	1791.21	466.391	1446.27	143.22	1.919	2354	2523.81	0.770	3.086	0.087	1.409	1.314	0.010	2.038	17.791
BHJC	2129.46	483.886	1889.10	172.51	2.294	2771	3005.45	0.773	2.936	0.072	1.411	1.301	0.011	2.666	19.901

The parameter analysis in sixth-order catchments incurs, however, in a homogenization and generalization of their susceptibility to fluvial flooding, hiding internal differences that may occur due to hydrogeomorphological differences along the catchments. Thus, based on the drainage stream ordering of the BHSM and BHJC, 3941 first-order, 896 second-order, 207 third-order, 53 fourth-order, and 13 fifth-order sub-catchments were obtained (Table 5). However, for the purpose of morphometric susceptibility analysis, as presented in the methodology of this paper, the parameters of the first- and second-order sub-catchments were not analyzed.

Table 5. Number of third- to sixth-order sub-catchments and percentage of the total catchment area for each stream-order.

	BHSM	% of the area	BHJC	% of the area
Third-order	93	64.97%	114	59.48%
Fourth-order	23	63.53%	30	73.01%
Fifth-order	6	56.83%	7	59.77%
Sixth-order	1	100%	1	100%

4.2. Morphometric susceptibility in fifth- and fourth-order catchments

In fifth-order catchments, a distinction in the susceptibility pattern occurs, in which the highest values are concentrated in the drainage divides to the south of the BHJC. The morphometric parameters A (425.1 km²; 379.1 km²; 182.9 km²), P (169.1 km; 195.8 km; 121.6 km), R (1173.6 m; 1836.5 m; 901.3 m), Lm (51.1 km; 74.5 km; 29.5 km), Nu (569; 484; 221), Lu (584.1 km; 528.7 km; 257.1 km) and Kc (2.297; 2.816; 2.518) for the 5JC5, 5JC6 and 5JC7 catchments, respectively, were decisive in determining their susceptibility to fluvial flooding, placing them in the upper quartile as they possess cumulative values above 41 (Figure 5).

The 5SM4, 5SM5 and 5JC4 catchments belong to the third quartile, with cumulative values of 39, 35 and 41, respectively, followed by the 5SM2, 5SM6 and 5JC3 catchments, with 33, 36 and 33, respectively. The fifth-order catchments with the lowest morphometric susceptibility to fluvial flooding have cumulative values below 32: 5SM1, 5SM3, 5JC1 and 5JC2.

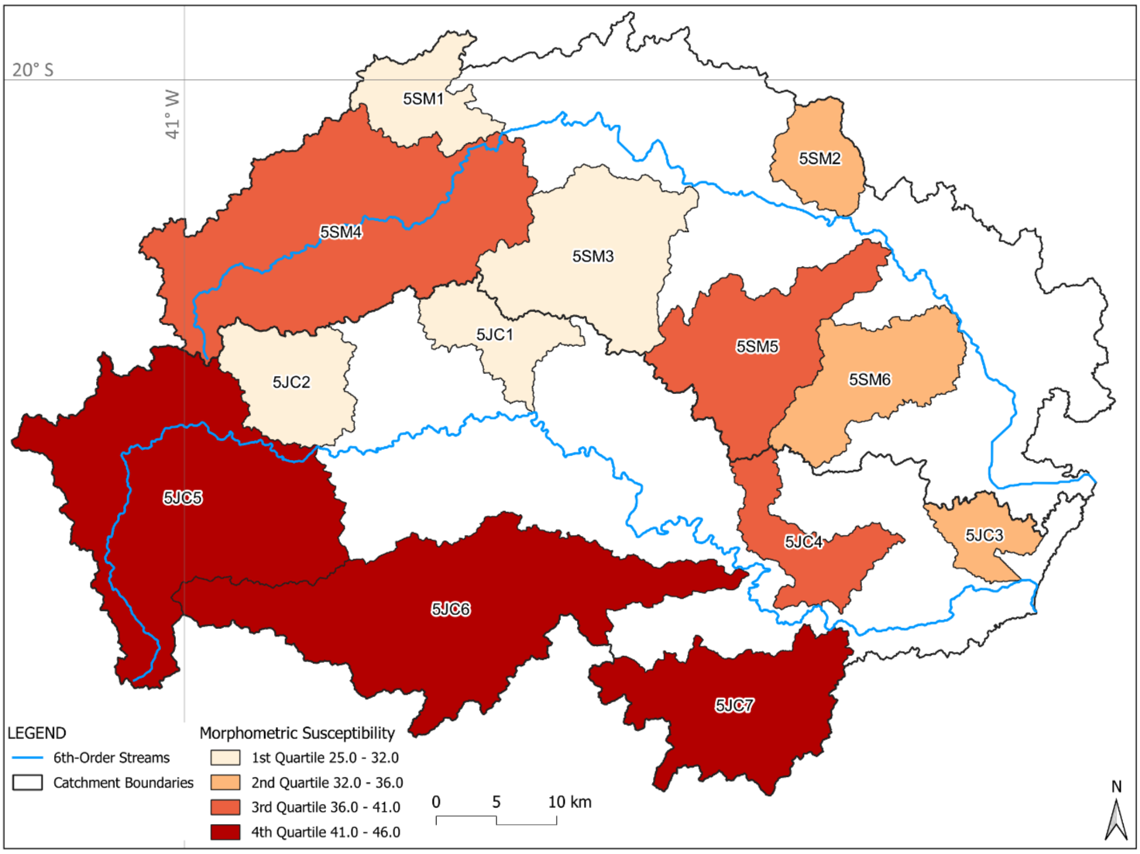

Figure 5. Morphometric susceptibility to fluvial flooding in fifth-order sub-catchments. Map prepared by the author.

The detailing of susceptibility in fourth-order catchments demonstrates that there is an important correlation with the degree of susceptibility in catchments of the immediately higher stream-order, corroborating the premise that hierarchical delineation and analysis at the sub-catchment level are fundamental for the spatial assessment of hydrological responsiveness and for the identification of homogeneous risk areas (Souza, 2005). An example can be observed in the catchments to the south of the BHJC that remain with high cumulative values, while fourth-order sub-catchments of low morphometric susceptibility are spatially distributed in association with fifth-order sub-catchments that also possess low susceptibility, or previously unclassified areas.

It is noted that, in the mapping of fifth-order catchments, 41.6% of the area was not classified, whereas in fourth-order catchments this percentage decreased to 31.2%, reflecting the existence of fourth-order sub-catchments draining directly into sixth-order channels (Figure 6). A total of 13.9% of the area that comprised fifth-order catchments of the upper quartile remained with the same classification in the analysis of fourth-order catchments, which reflects a concentration of morphometric conditions prone to the development of fluvial flooding in these areas, confirming that the detailed spatial assessment of these parameters is critical for the prediction and identification of specific sites highly susceptible to fluvial flooding (Tola; Shetty, 2022; Servidoni et al., 2023).

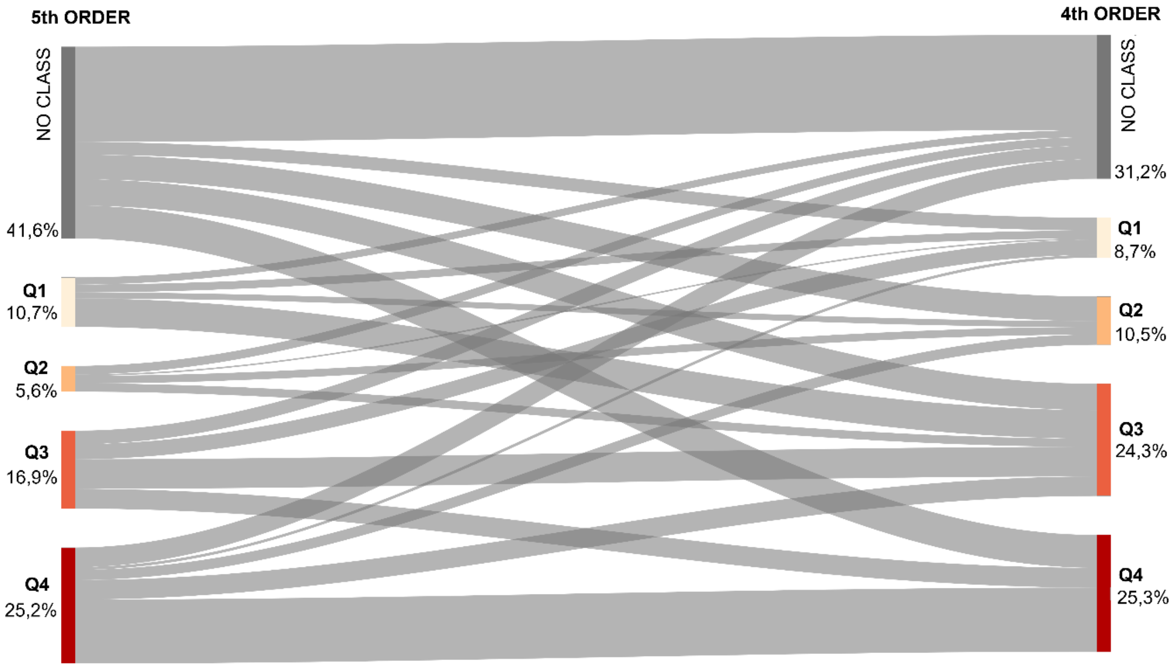

Figure 6. Representation of the spatial transition (area) of the morphometric susceptibility quartiles from fifth-order catchments to fourth-order catchments. In the diagram, the percentage represents the total area occupied by the catchments of each quartile in relation to the study area.

Among the fourth-order sub-catchments with the highest degree of susceptibility to fluvial flooding are those that possess cumulative values above 42. In the upper quartile, there are 12 sub-catchments, of which only 3 (4SM17; 4SM19; 4SM21) are located in the BHSM (Figure 7). The sub-catchments with the highest morphometric susceptibility follow the same pattern with high values of A, P, R, Nu, Lu, and Rn, whereas the other parameters show greater variation, such as the parameters F, Fs, and Dd.

The 13 sub-catchments of the third quartile possess cumulative values between 38 and 42, among which 8 are located in the BHSM and 5 in the BHJC. It is noted that smaller catchments are found in this quartile, such as 4SM20 and 4SM13, with cumulative values of 38 and 40, respectively, which have high susceptibility to fluvial flooding due to the steep slope and parameters such as Tc, Dd, Fs, and Rr. This finding is corroborated by the literature, which demonstrates that the combination of steep slopes (high Rr), high drainage network density, and short Tc are the primary causes for the acceleration of surface runoff and generation of peak flows (Ali et al., 2023; Tola; Shetty, 2022). Among the sub-catchments of the third quartile, 5 are located in the BHSM whereas 8 are located in the BHJC. The sub-catchments of the lower quartile gather cumulative values between 24 and 32 and are concentrated along the left bank of the BHJC, whereas in the BHSM the sub-catchments of this quartile are located in higher elevation areas of the catchment.

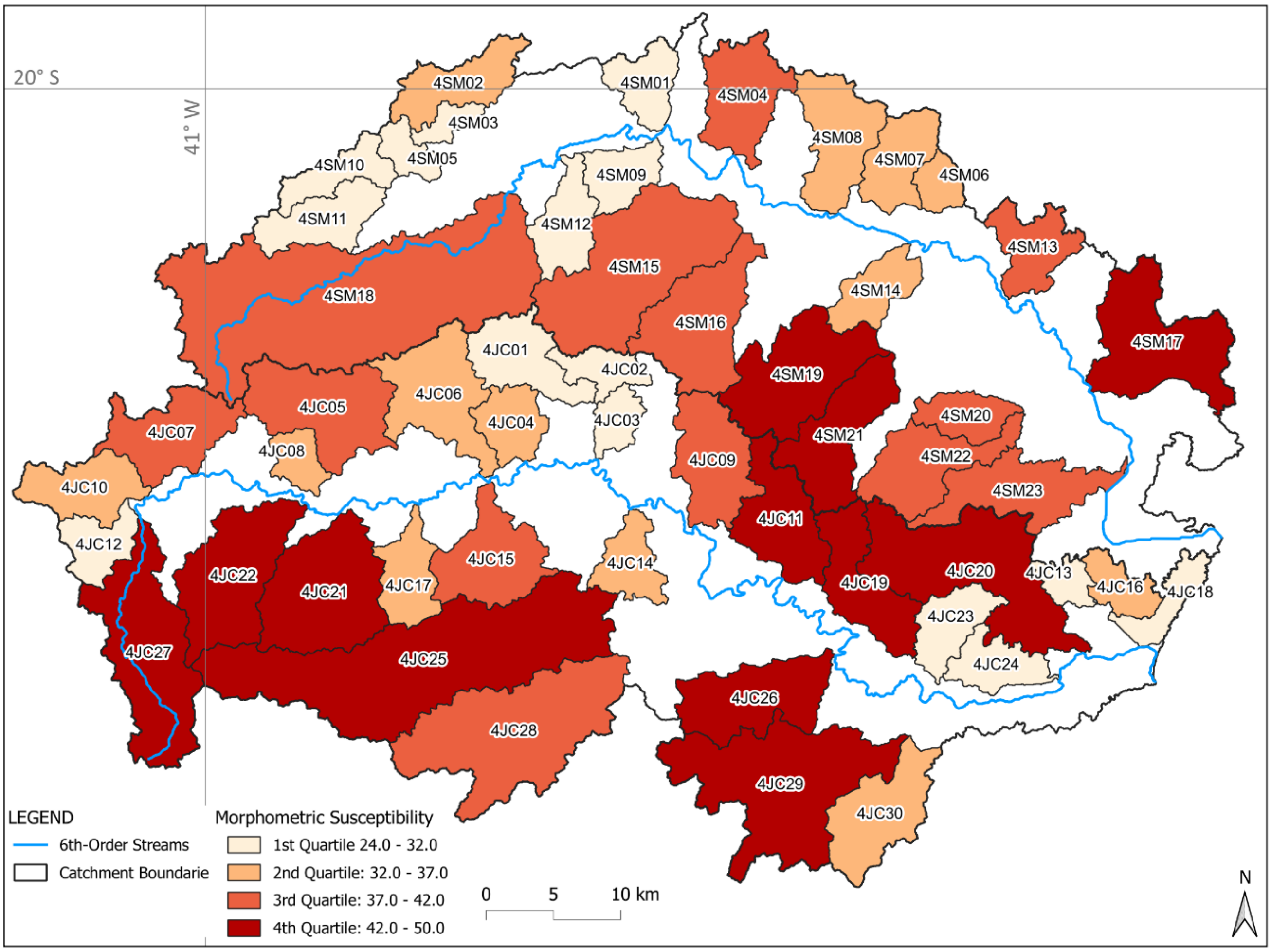

Figure 7. Morphometric susceptibility map to fluvial flooding in fourth-order sub-catchments. Map prepared by the author.

4.3. Susceptibility to fluvial flooding in third-order catchments

The third-order sub-catchments possess dimensions ranging from 2.4 km² to 54.6 km² and are irregularly distributed throughout the study area. At this level of morphometric susceptibility detailing, it is possible to identify the contribution level that each sub-catchment has in the generation of fluvial flooding, forming a more detailed mosaic of the fluvial flooding susceptibility potential to which the population residing in these areas is subjected.

There is a higher concentration of sub-catchments more susceptible to fluvial flooding near the drainage divide between the BHSM and BHJC, which is not necessarily associated with their mean elevation (Figure 8A), whereas the less susceptible ones do not present a well-defined spatial pattern. However, it is notable that the catchments in the upper quartile possess parameters associated with their dimension, generating a greater influence on the susceptibility classification, with emphasis on the sub-catchments of the right bank of the BHSM. The hydrogeomorphological literature confirms that the absolute size of the catchment is a primary conditioning factor, since it dictates the amount of captured excess rainfall and the response time, influencing the development of fluvial flooding (Souza, 2005).

In addition to the parameters associated with the catchment area (Figure 8B), there is also a positive correlation between the degree of susceptibility and the relief of the third-order sub-catchments (Figure 8C), indicating an important influence on the runoff velocity. In fact, it is understood that a greater altimetric amplitude acts by increasing the energy gradient of the waters, which induces faster flows, significantly shortens the concentration time, and intensifies the surface runoff peaks (Dutal, 2023; Tola; Shetty, 2022).

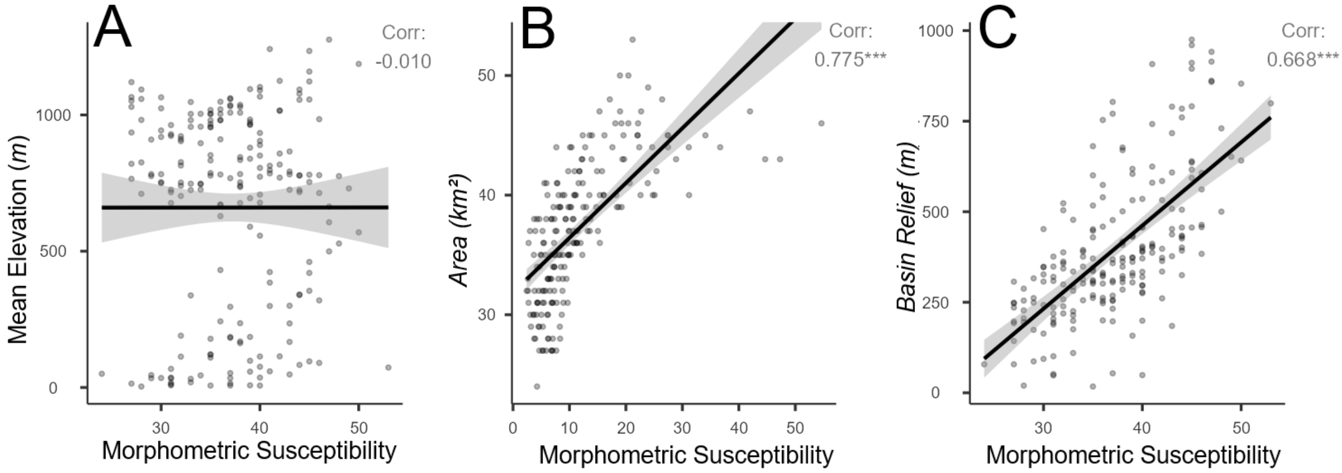

Figure 8. Correlation (Spearman) between morphometric susceptibility and the parameters of (A) mean elevation (Rho -0.010), area (A) (Rho 0.775), and (C) basin relief (Rho 0.668) of the third-order sub-catchments.

The cumulative morphometric susceptibility values range from 24 to 53, with a higher frequency near the median, indicating a distribution closer to normal, whereas extreme values present a lower frequency and greater variation (Figure 9). Among the sub-catchments belonging to the lower quartile, 29 are located in the BHSM, whereas 30 are located in the BHJC. Among the 48 belonging to the second quartile, there is a greater concentration in the BHJC with 29 sub-catchments. The third quartile also concentrates most of the sub-catchments in the BHJC, with 29 out of the 50. The sub-catchments of the upper quartile, with higher susceptibility, possess greater variation, with values between 41 and 53, and are concentrated in the BHSM.

It is important to highlight that larger catchments also tend to receive a greater volume of precipitation, while, on the other hand, they possess a greater attenuation capacity due to high values of Tc (Bajabaa; Masoud; Al-Amri, 2014). However, the Relief (R) associated with these areas and the higher channel slope value can lead to lower infiltration and higher associated surface runoff, raising the potential for sudden fluvial flooding in steeper sub-catchments.

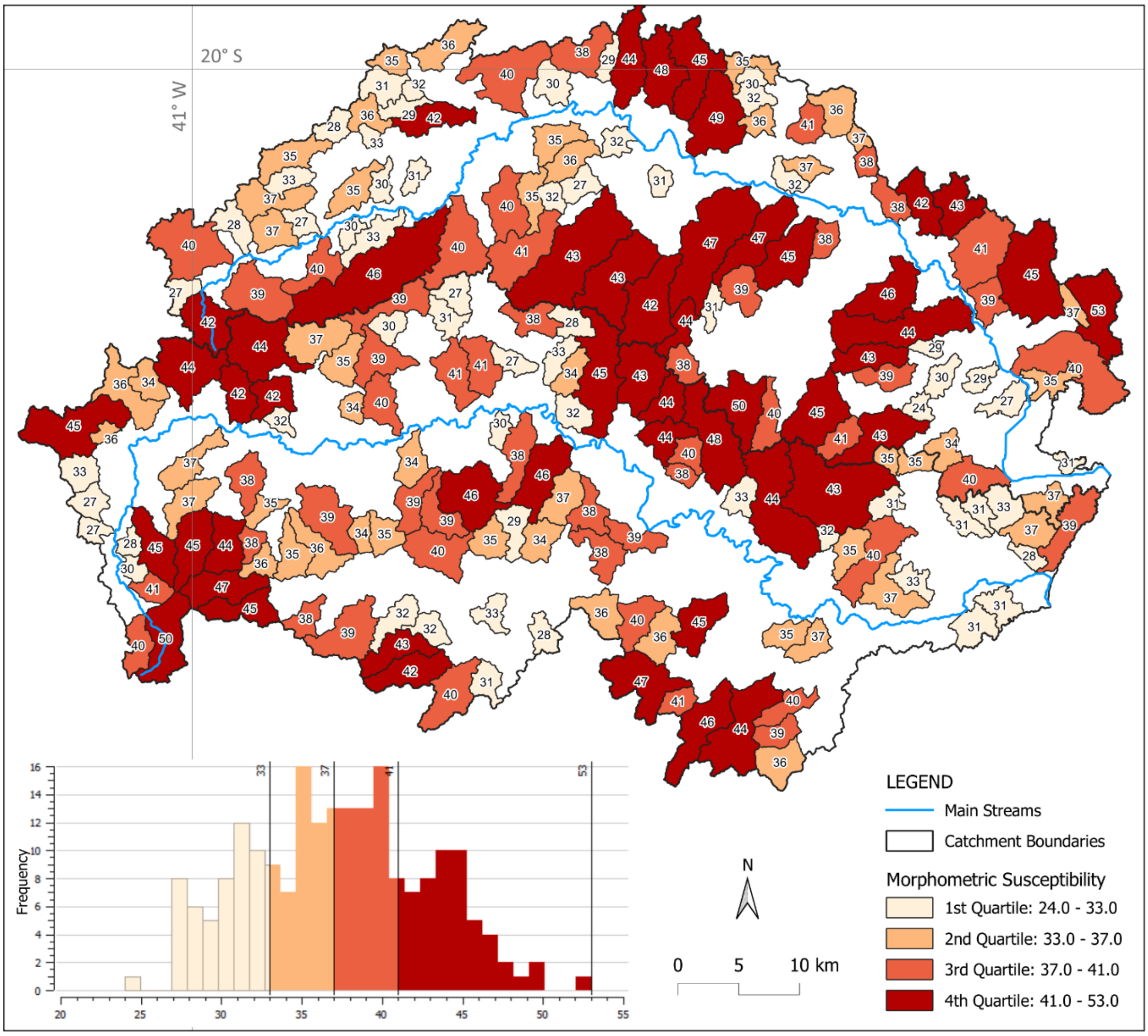

Figure 9. Morphometric susceptibility map to fluvial flooding in third-order sub-catchments and distribution graph of the value counts in the histogram. Map prepared by the author.

4.4. Fluvial flooding susceptibility zoning

The mean annual precipitation in the study area ranges between 973 and 1933 mm yr⁻¹. However, the BHJC possesses a greater range, whereas the BHSM concentrates its values near the median (1392 mm yr⁻¹). Even with minor variations in the maximum and minimum values, both possess similarities given the geomorphological and climatic context prone to the development of orographic rainfall, since the presence of mountain massifs and escarpments near the coast acts as an orographic barrier to the circulation of humid fronts, increasing rainfall volumes in the highest parts (Souza, 2005; Nascimento, 2017; Servidoni et al., 2023). However, the literature consolidates that rainfall incidence, although acting as a triggering mechanism, is not the sole determinant of the hydrogeomorphological system's criticality (Mendiondo; Tucci, 1997). When dealing with small and mountainous catchments, the high topographic ruggedness and steep slopes drastically reduce the time of concentration, accelerating the conversion of the climatic input into surface runoff and establishing the dominance of the relief over the hydrological dynamics (Hallema et al., 2016; Freitas, 2018).

This premise is empirically demonstrated by the precipitation distribution against the susceptibility of these sub-catchments. Figure 10 presents a slight tendency of increasing precipitation medians towards the upper quartiles of third-order sub-catchments; however, it is accompanied by an expressive overlap of the ranges and interquartile ranges among all classes (Q1 to Q4). In the BHJC, for instance, the highest hazard quartile (Q4) presents a median comparable to that of Q3, but exhibits the greatest sample dispersion, with volumes ranging from values close to 1000 mm yr⁻¹ to the absolute maximum ceiling. This statistical behavior provides evidence that spatial units subjected to equivalent rainfall loads can be framed into diametrically opposed degrees of susceptibility (from Q1 to Q4). The absence of an isolation of the highest rainfall volumes restricted to the highest hazard level demonstrates that the degree of susceptibility to fluvial flooding is not solely governed by the water surplus. Such evidence reaffirms that the integration of the spatial distribution of rainfall acts to spatialize the climatic trigger (Tola; Shetty, 2022), proving to be essential precisely because the morphological and topographic arrangement acts decisively in the amplification or mitigation of this local runoff (Lavarini; Magalhães Júnior, 2013).

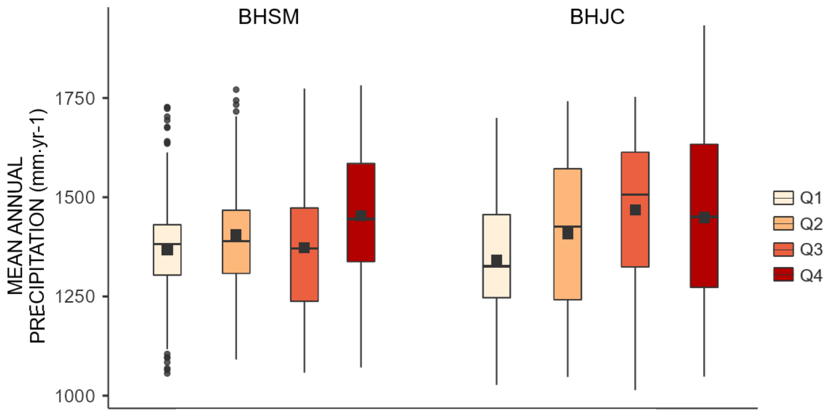

Figure 10. Distribution of the mean annual precipitation based on CHELSA v.1.2 as a function of the quartiles of morphometric susceptibility to fluvial flooding for the third-order catchments. Prepared by the author.

By combining the mean precipitation values of each sub-catchment up to the sixth-order with the obtained morphometric susceptibility, it was possible to generate a synthesis map with the susceptibility to fluvial flooding classes in the study area (Figure 11A). In order to cover the entire area, the results obtained for each hierarchical order were overlaid, such that the third-order sub-catchments overlay the other classes, followed by fourth-, fifth-, and sixth-order sub-catchments (Figure 11B). In this overlay, there was no reclassification of the morphometric susceptibility values, so that each class remained classified according to its stream order.

When comparing the dimensionless parameters such as Si, F, Kc, Dd, Fs, Rr, Rn, and Tc of the sixth-order catchments to the values found for them in fifth-order catchments, it was observed that the BHSM and BHJC both possess values that indicate a very high morphometric potential to generate fluvial flooding. The integrated analysis of these parameters proves to be fundamental to identify the hydrological behavior of a catchment, specifically the clustering of high values of Dd and Fs, allied to specific form factors such as Kc and F, which indicate a high propensity for the rapid concentration of surface runoff and point to a hydrological behavior prone to the generation of severe fluvial flooding (Servidoni et al., 2023)."

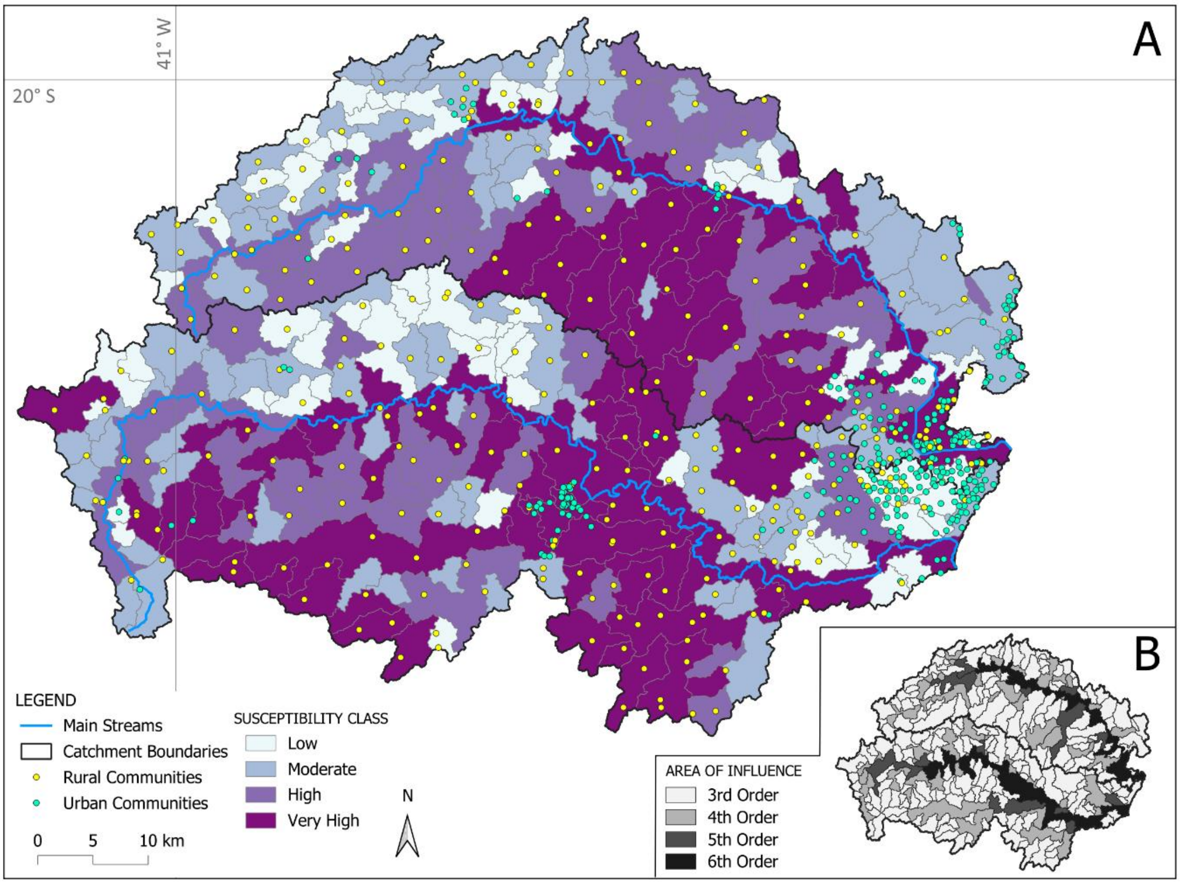

Figure 11. Synthesis map with (A) Distribution of the susceptibility classes to fluvial flooding considering the morphometric susceptibility values and the mean precipitation for each sub-catchment; (B) Overlay of third- to sixth-order sub-catchments. Map prepared by the author.

As a result of the assessment, areas with very high susceptibility were found in both catchments, especially in the middle course of the BHSM and along the right bank of the BHJC, representing, respectively, 32.6% and 43.7% of the catchment area. In these areas of higher susceptibility, 213 urban and rural communities are located (IJSN, 1994), belonging to the municipalities of Santa Leopoldina, Santa Maria de Jetibá, Domingos Martins, Marechal Floriano, Vila Velha, Cariacica, Guarapari, and Vitória. The areas of high susceptibility comprise 28.9% of the BHSM and 20.0% of the BHJC and encompass 99 communities.

The areas of moderate susceptibility are fragmented in both catchments and encompass 166 urban and rural communities. The coverage area of this class corresponds to 27.2% of the BHSM and 21.6% of the BHJC. The catchments of low susceptibility, in turn, possess the lowest area percentage with 11.3% and 14.7%, respectively, and encompass 80 urban and 50 rural communities.

5. Conclusions

The results reinforce the relevance of morphometric parameters, such as the A and the R, as well as correlated attributes, the P and main channel slope, in defining areas more susceptible to fluvial flooding. In a mountainous setting, the geomorphological context proves to be the dominant factor in the hydrological dynamics over the absolute precipitation amounts. It is necessary to highlight that, although the predominantly elongated shapes of these sub-catchments tend to favor the translation and attenuation of the flow, the small dimensions and the extremely steep slopes and topographic ruggedness supplant this morphological attenuation, drastically accelerating the surface runoff.

Besides the morphometric characteristics of the BHSM and BHJC, the consideration of the topographic effects at the sub-catchment level, classified based on their stream-order, enabled a detailing that until then had not been performed for the study area, providing a more precise local analysis of areas more susceptible to fluvial flooding.

In both catchments, a significant percentage of areas with very high susceptibility was identified, which converges with the local history of these events. In the BHSM, the most susceptible areas are concentrated in the middle and lower courses, whereas in the BHJC these areas, which comprise most of the catchment, are better distributed. However, the predominance of more susceptible areas on the right bank of the main channels of both catchments is a strong indication that the drainage axis, convex to the North, may have generated an asymmetry in the morphometric configuration of the sub-catchments, generating a greater potential for fluvial flooding on the right bank.

The identified morphometric susceptibility points to areas more prone to natural fluvial flooding. However, risk managers must consider that alterations in fluvial systems, such as soil sealing and channelization in urbanized areas, can generate hydrological distortions that significantly amplify peak flows and the severity of the events. In this sense, the main contribution of this study relies on the methodological robustness of the multiscale analysis, down to the third-order, for the regionalization of risk areas, overcoming the homogenization limitation inherent to macroscale studies and providing more precise mapping in a scenario of hydrological data scarcity in channels of lower stream-order. The achieved results guide the territorial planning and the development of fluvial flooding mitigation policies for the study area, offering a critical analytical basis for understanding the hydrogeomorphological vulnerability in the contact zone between the mountainous belt and the coastal plain.

Author's contributions: Conceptualization, M.V.O.S and A.P.M.J.; methodology, M.V.O.S and A.P.M.J.; validation, M.V.O.S and A.P.M.J.; formal analysis, M.V.O.S; investigation, M.V.O.S; resources, M.V.O.S; data curation, M.V.O.S; writing—original draft preparation, M.V.O.S and A.P.M.J.; writing—review and editing, M.V.O.S and A.P.M.J. All authors have read and agreed to the published version of the manuscript.

Funding: This research was funded by the Fundação de Amparo à Pesquisa do Estado de Minas Gerais – FAPEMIG, through a doctoral fellowship granted in the year 2022/2023 to the first author. Grant number 5.18/2022.

Acknowledgments: The authors thank the Graduate Program in Geography of the UFMG and the CNPq for the PQ fellowship 317019/2025-2 granted to professor Antônio Pereira Magalhães Júnior.

Conflicts of Interest: The authors declare no conflicts of interest.

Declaration of Artificial Intelligence Use: During the preparation of this manuscript, the authors used the Gemini 1.5 Pro tool with the objective of improving the grammar and fluency of the text and assisting in the translation into English. After using the tool, the authors critically reviewed and edited all content, assuming full and integral responsibility for the published manuscript, including any potential inaccuracies or errors.

References

1. ABDEL-FATTAH, M.; SABER, M. KANTOUSH, S. A.; KHALIL, M. F.; SUMI, T.; SEFELNASR, A. M. A hydrological and geomorphometric approach to understanding the generation of wadi flash floods. **Water**, v. 9, n. 7, p. 553, 2017. DOI: 10.3390/w9070553
2. ABUZIED, S.; YUAN, M.; IBRAHIM, S.; KAISER, M.; SALEEN, T. Geospatial risk assessment of flash floods in Nuweiba area, Egypt. **Journal of Arid Environments**, v. 133, p. 54-72, 2016. DOI: 10.1016/j.jaridenv.2016.06.004
3. ADNAN, M. S. G.; ABDULLAH, A. Y. M.; DEWAN, A.; HALL, J. W. The effects of changing land use and flood hazard on poverty in coastal Bangladesh. **Land Use Policy**, n. 99. 2020. DOI: 10.1016/j.landusepol.2020.104868
4. ALAM, A.; AHMED, B.; SAMMONDS, P. Flash flood susceptibility assessment using the parameters of drainage basin morphometry in SE Bangladesh. **Quaternary International**, v. 575, p. 295-307, 2021. DOI: 10.1016/j.quaint.2020.04.047
5. ALI, M. A. S.; SARWAR, A.; ALI, M.; GULZAR, S.; MAJID, A.; KHAN, M. I.; NAZIR, J.; AHMAD, A. Application of Morphometric Ranking Approach using Geospatial Techniques for Flash Flood Susceptibility Modelling in District Shangla, Pakistan. **Proceedings of the Pakistan Academy of Sciences**: **B. Life and Environmental Sciences**, 60, n. 2 , 243-255, 2023. DOI: 10.53560/PPASB(60-2)830
6. ALMEIDA, F. F. M. o Cráton do São Francisco. **Revista Brasileira de Geociências**, São Paulo, v.7, p. 249-264, 1977. DOI: 10.25249/0375-7536.1977349364
7. ANTONGIOVANNI L. L.; COELHO A. L. N. **Panorama sobre a desertificação no estado do Espírito Santo**. Consultoria e relatório apresentados para o IEMA do Governo do Estado do Espírito Santo. MMA, Brasília. 87p. 2005.
8. BAJABAA, S.; MASOUD, M.; AL-AMRI, N. Flash flood hazard mapping based on quantitative hydrology, geomorphology and GIS techniques (case study of Wadi Al Lith, Saudi Arabia). **Arabian Journal of Geosciences**, v. 7, p. 2469-2481, 2014. DOI: 10.1007/s12517-013-0941-2

9. BHAT, M. S.; AHMAD, A. A. S.; FAROOQ, H. AHMAD, B. Flood hazard assessment of upper Jhelum basin using morphometric parameters. **Environmental Earth Sciences**, v. 78, p. 1-17, 2019. DOI: 10.1007/s12665-019-8046-1
10. BHATT, S.; AHMED, S. A. Morphometric analysis to determine floods in the Upper Krishna basin using Cartosat DEM. **Geocarto international**, v. 29, n. 8, p. 878-894, 2014. DOI: 10.1080/10106049.2013.868042
11. BORGA, M.; GAUME, E.; CREUTIN, J. D.; MARCHI, L. Surveying flash floods: gauging the ungauged extremes. **Hydrological Processes**, v.22, n.18, p. 3883–3885. 2008. DOI: 10.1002/hyp.7111
12. CALEGARI, S. S.; PEIFER, D.; NEVES, M. A.; CAXITO, F. Post-Miocene topographic rejuvenation in an elevated passive continental margin not characterized by a sharp escarpment (northern end of the Mantiqueira Range, Brazil). **GEOMORPHOLOGY**, v. 393, 2021. DOI: 10.1016/j.geomorph.2021.107946
13. CARVALHO, L. M. V. de; JONES, C. Zona de Convergência do Atlântico Sul. In: CAVALCANTI, I. F. de A; FERREIRA, N. J; SILVA, M. G. A. J. da; DIAS, M. A. F. da. **Tempo e Clima no Brasil.** São Paulo: Oficina de Textos, 2009. (p. 95-109).
14. CHEREM, L. F. S. **Análise morfométrica da Bacia do Alto Rio das Velhas – MG**. Dissertação (Mestrado em Análise e Modelagem de Sistemas Ambientais) – Instituto de Geociências, Universidade Federal de Minas Gerais, Belo Horizonte, 2008. 111 p.
15. CHRISTOFOLETTI, A. **Geomorfologia**. São Paulo: Edgard Blücher, 1980.
16. CHRISTOFOLETTI, A. **Modelagem de sistemas ambientais**. Editora Blucher, 1999.
17. COSTA, J. E. Hydraulics and basin morphometry of the largest flash floods in the conterminous United States. **Journal of hydrology**, v. 93, n. 3-4, p. 313-338, 1987. DOI: 10.1016/0022-1694(87)90102-8
18. D'ALCÂNTARA, E, A. **Ensaios Sobre os Alagamentos do Município de Vila Velha**. 2012. Disponível em: http://www.morrodomoreno.com.br/materias/ensaios-sobre-os-alagamentosdo-municipio-de-vila-velha-.html Acesso em: mai, 2024.
19. DEINA, M. A.; COELHO, A. L. N. A Influência da Zona Convergência do Atlântico Sul (ZCAS) nos Eventos de Inundação no Baixo Jucu em Vila Velha (ES). **Geografia (Londrina)**, v. 24, n. 2, p. 05-23, 2015. DOI: 10.5433/2447-1747.2015v24n2p05
20. DUTAL, H. Using morphometric analysis for assessment of flash flood susceptibility in the Mediterranean region of Turkey. **Environmental monitoring and assessment**, v. 195(5), n. 582, 2023. DOI: 10.1007/s10661-023-11201-0
21. FENTA, A. A.; YASUDA, H.; SHIMIZU, K.; HAREGEWEYN, N.; WOLDEAREGAY, K. Quantitative analysis and implications of drainage morphometry of the Agula watershed in the semi-arid northern Ethiopia. **Applied Water Science**, v. 7, p. 3825-3840, 2017. DOI: 10.1007/s13201-017-0534-4
22. FREITAS, A. R. de. **Identificação de áreas potencializadoras de inundações e enxurradas**: uma proposta metodológica aplicada na Bacia Arroio dos Pereiras, Irati-PR. Tese (Doutorado em Geografia) – Universidade Estadual de Ponta Grossa, Ponta Grossa, 2018. 150 p.
23. GUTH, P. L.; GEOFFROY, T. M. LiDAR point cloud and ICESat-2 evaluation of 1 second global digital elevation models: Copernicus wins. **Transactions in GIS**, v. 25, n. 5, p. 2245-2261, 2021. DOI: 10.1111/tgis.12825
24. HALLEMA, D. W.; MOUSSA, R.; SUN, G. McNULTY, S. G. Surface storm flow prediction on hillslopes based on topography and hydrologic connectivity. **Ecological Processes**, v. 5, n. 1, p. 13, 2016. DOI: 10.1186/s13717-016-0057-1
25. HORTON, R. E. Drainage-basin characteristics. **Transactions, American Geophysical Union**, V. 13, n. 1, p. 350-361, 1932. DOI: 10.1029/TR013i001p00350
26. HORTON, R. E. Erosional development of streams and their drainage basins; hydrophysical approach to quantitative morphology. **Geological society of America bulletin**, v. 56, n. 3, p. 275-370, 1945. DOI: 10.1130/0016-7606(1945)56[275:EDOSAT]2.0.CO;2
27. IBGE – Instituto Brasileiro de Geografia e Estatística; **Geografia do Brasil**: Região Sudeste. V.3. Rio de Janeiro: IBGE, 1977.
28. IJSN – Instituto Jones dos Santos Neves. Nota Técnica e Arquivos Vetoriais – **Projeto Mapeamento de Comunidades Urbanas e Rurais do Espírito Santo** – Divisão Territorial. 1994. Disponível em: https://geobases.es.gov.br/links-para-mapas Acesso em: outubro de 2024.
29. INCAPER - Instituto Capixaba de Pesquisa, Assistência Técnica e Extensão Rural. **Gráficos da Série Histórica**. Disponível em: < https://meteorologia.incaper.es.gov.br/graficos-da-serie-historica>. Acesso em: nov. 2023.
30. INMET - Instituto Nacional de Meteorologia. **Eventos Extremos de Março de 2024 No Brasil**. Notícias Técnicas. Brasília/DF. 2024. Disponível em: https://portal.inmet.gov.br/notasTecnicas# Acesso em: mai. 2024.
31. IPCC - Intergovernmental Panel on Climate Change. **Synthesis Report of the IPCC Sixth Assessment Report (AR6)**. 2021. Disponível em: - https://www.ipcc.ch/report/sixth-assessment-report-cycle/ Acesso em: maio de 2023.
32. KARGER, D. N.; CONRAD, O.; BÖHNER, J.; KAWOHL, T.; KREFT, H.; SORIA-AUZA, R.W.; ZIMMERMANN, N. E.; LINDER, H. P.; KESSLER, M. Climatologies at high resolution for the earth's land surface areas. **Scientific Data,** v.4, n.1, p.1-20. 2017. DOI: 10.1038/sdata.2017.122
33. KIRPICH, Z. P. Time of concentration of small agricultural watersheds. **Civil engineering**, v. 10, n. 6, p. 362, 1940.

34. LAVARINI, C.; MAGALHÃES JÚNIOR, A. P. Análise morfométrica de bacias de cabeceira como ferramenta de investigação geomorfológica em média e larga-escala espacial. Revista Brasileira de Geomorfologia, v. 14, n. 1, p. 35-46, jan./mar. 2013
35. MAGALHÃES JÚNIOR, A. P.; LOPESF. W. de A. **Recursos hídricos: as águas na interface sociedade-natureza**. Oficina de Textos, 2022.
36. MENDIONDO, E. M.; TUCCI, C. E. M. Escalas hidrológicas I: conceitos. **Rbrh: Revista Brasileira de Recursos Hídricos.** Porto Alegre, RS. vol. 2, n. 1, p. 59-79, 1997. DOI: 10.21168/rbrh.v2n1.p59-79
37. MILLER, V. C. A Quantitative Geomorphic Study of Drainage Basin: Characteristics in the Clinch Mountain Area Virginia and Tennessee. **Technical Report** (2). Columbia Univ New York, 1953.
38. MORISAWA, M. E. Quantitative geomorphology of some watersheds in the Appalachian Plateau. **Geological Society of America Bulletin**, v. 73, n. 9, p. 1025-1046, 1962. DOI: 10.1130/0016-7606(1962)73[1025:QGOSWI]2.0.CO;2
39. NASCIMENTO, F. H. do. **Análise do Efeito Orográfico na Distribuição de Chuvas**: estudo de caso nos municípios de Fundão e Santa Teresa (ES) no ano hidrológico (AH) 2015-2016. Dissertação (Mestrado em Geografia) – Universidade Federal do Espírito Santo, Vitória/ES, 2017. 154 p.
40. NUNES, L. H.; VICENTE, A. K.; CANDIDO, D. H. **Clima da região Sudeste do Brasil**. In: CAVALCANTI, I. F. A.; FERREIRA, N. J.; SILVA, M. G. A. J.; DIAS, M. A. F. S.; Orgs. Tempo e clima no Brasil. São Paulo: Oficina de Textos, p. 243-58, 2009.
41. OZDEMIR, H.; BIRD, D. Evaluation of morphometric parameters of drainage networks derived from topographic maps and DEM in point of floods. **Environmental geology**, v. 56, p. 1405-1415, 2009. DOI: 10.1007/s00254-008-1235-y
42. PATTON, P. C.; BAKER, V. R. Morphometry and floods in small drainage basins subject to diverse hydrogeomorphic controls. **Water resources research**, v. 12, n. 5, p. 941-952, 1976. DOI: 10.1029/WR012i005p00941
43. PINTO, V. G.; LIMA, R. N. S.; SANTOS, R. C. P.; RIBEIRO, C. B. M. Influência do número de classes de vulnerabilidade na determinação da suscetibilidade morfométrica à inundação. **Ambiente & Água - An Interdisciplinary Journal of Applied Science**, Taubaté, v. 11, n. 3, p. 637-649, 2016. DOI: 10.4136/ambi-agua.1842
44. QGIS Development Team. **QGIS Geographic Information System (versão 3.22)**. 2022. Disponível em: <http://qgis.osgeo.org>.
45. RAZALI, N. M.; WAH, Y. B. Power comparisons of shapiro-wilk, kolmogorov-smirnov, lilliefors and anderson-darling tests. **Journal of statistical modeling and analytics**, v. 2, n. 1, p. 21-33, 2011.
46. RENTSCHLER, J.; MARCONCINI, M.; SU, R.; STRANO, E.; BERNARD, L.; HALLEGATTE, S.; RIOM, C.; AVNER, P. Rapid Urban Growth in Flood Zones: Global Evidence since 1985. **Policy Research Working Paper**; 10014. World Bank, Washington, DC. World Bank. 2022. Disponível em: https://openknowledge.worldbank.org/handle/10986/37348. Acesso em: Jun. 2024.
47. ROMSHOO, S. A.; BHAT, S. A.; RASHID, I. Geoinformatics for assessing the morphometric control on hydrological response at watershed scale in the Upper Indus Basin. **Journal of Earth System Science**, v. 121, p. 659-686, 2012. DOI: 10.1007/s12040-012-0192-8
48. SCHUMM, Stanley A. Evolution of drainage systems and slopes in badlands at Perth Amboy, New Jersey. **Geological society of America bulletin**, v. 67, n. 5, p. 597-646, 1956. DOI: 10.1130/0016-7606(1956)67[597:EODSAS]2.0.CO;2
49. SCHWANGHART, W.; SCHERLER, D. TopoToolbox 2-MATLAB-based software for topographic analysis and modeling in Earth surface sciences. **Earth Surface Dynamics**, v. 2, n. 1, p.1-7. 2014. DOI: 10.5194/esurf-2-1-2014
50. SERVIDONI, L. E.; SANTANA, D. B.; LENSE, G. H. E.; PARREIRAS, T. C.; AYER, J. E. B.; RUBIRA, F. G.; MINCATO, R. L. Detection of vulnerable areas to the occurrence of floods in tropical regions, from morphometric attributes. **Revista Brasileira de Geomorfologia**, v. 24, n. 4, 2023. DOI: 10.20502/rbgeomorfologia.v24i4.2287
51. SHAPIRO, S. S.; WILK, M. B. An analysis of variance test for normality (complete samples). **Biometrika**, 52(3-4), 591–611. 1965. DOI: 10.2307/2333709
52. SILVA, A. C. **Histórico de desastres do estado do Espírito Santo 2000-2009**. Defesa Civil do Estado do Espírito Santo. Grafitusa Gráfica e Editora, 2010. Disponível em: https://defesacivil.es.gov.br/publicacoes-2 Acesso em: maio de 2024.
53. SILVA, R. M. J.; LIMA, C. I. M.; VERONESE, V. F.; JUNIOR, R. N. R.; ROCHA, M. R.; JUNIOR, S. O. Geologia. **Projeto Radam Brasil**. Folhas se 24 Rio Doce, v.34. Rio de Janeiro, 1987.
54. SILVA, K. R. da.; CECÍLIO, R. A.; XAVIER, A. C.; PEZZOPANE, J. R. M.; GARCIA, G. de O. Interpolação espacial da precipitação no Estado do Espírito Santo. **Floresta e Ambiente**, v. 18, p. 417-427, 2011. DOI: 10.4322/floram.2011.061
55. SIRANGELO, F. R. **Relação entre a ocorrência de inundações e enxurradas e os índices morfométricos das sub-bacias hidrográficas da Região Hidrográfica do Guaíba, Rio Grande do Sul, Brasil**. Dissertação (Mestrado em Sensoriamento Remoto) – Universidade Federal do Rio Grande do Sul, Porto Alegre, 2014. 149 p.

56. SHEN, X.; ANAGNOSTOU, E. N.; MEI, Y.; HONG, Y. A global distributed basin morphometric dataset. **Scientific Data**, v. 4, n. 1, p. 1-8, 2017. DOI: 10.1038/sdata.2016.124
57. SMALL, Christopher; NICHOLLS, Robert J. A global analysis of human settlement in coastal zones. **Journal of coastal research**, p. 584-599, 2003.
58. SOUZA, Celia R. de G. Suscetibilidade morfométrica de bacias de drenagem ao desenvolvimento de inundações em áreas costeiras. **Revista Brasileira de Geomorfologia**, v. 6, n. 1, 2005. DOI: 10.20502/rbg.v6i1.38
59. STRAHLER, Arthur N. Hypsometric (area-altitude) analysis of erosional topography. **Geological society of America bulletin**, v. 63, n. 11, p. 1117-1142, 1952. DOI: 10.1130/0016-7606(1952)63[1117:HAAOET]2.0.CO;2
60. TEHRANY, M. S.; JONES, S.; SHABANI, F. Identifying the essential flood conditioning factors for flood prone area mapping using machine learning techniques. **Catena**, v. 175, p. 174-192, 2019. DOI: 10.1016/j.catena.2018.12.011
61. THE JAMOVI PROJECT. Jamovi. (Version 2.3) [Computer Software]. Retrieved from https://www.jamovi.org. 2022.
62. TOLA, S. Y.; SHETTY, A. Flood susceptibility modeling based on morphometric parameters in Upper Awash River basin, Ethiopia using geospatial techniques. **Sustainable Water Resources Management**, 8(2), 49, 2022. DOI: 10.1007/s40899-022-00642-z
63. VASCONCELLOS, F. C. **Variabilidade Atmosférica Associada a Casos Extremos de Precipitação na Região Sudeste do Brasil**. Dissertação (Mestrado em Meteorologia) Programa de pós-graduação em Meteorologia. Instituto Nacional de Pesquisas Espaciais, São José dos Campos, 2008. 110 p.
64. UNDRR – UN Office for Disaster Risk Reduction; CRED – Centre for Research on the Epidemiology of Disasters. **Human cost of natural disasters**: An overview of the last 20 years 2019-2020. 2020. Disponível em: https://reliefweb.int/report/world/human-cost-disasters-overview-last-20-years-2000-2019. Acesso em agosto de 2021.
65. WMO – World Meteorological Organization: Flash Flood Guidance System (FFGS) with global coverage Brochure. 2016.

This work is licensed under the Creative Commons License Atribution 4.0 Internacional (http://creativecommons.org/licenses/by/4.0/) – CC BY. This license allows for others to distribute, remix, adapt and create from your work, even for commercial purposes, as long as they give you due credit for the original creation.